CHAPTER VI
IMPROVING SELECTIVE PROPERTIES OF DPPV/(ZEOLITE Y, MORDENITE, 5A) AND RESPONSE TOWARDS CHEMICAL VAPORS

6.1 Abstract

In this work, doped poly(p-phenylene vinylene)/zeolite composites was prepared to detect the three different chemical vapors (acetone, methanol, and n-heptane) and to investigate the effects of zeolite type, chemical vapor type, and vapor concentration based on the electrical conductivity response and selectivity properties of the sensing materials. Zeolite Y (Si/Al=5.1 and Na$^+$), mordenite (Si/Al=18 and Na$^+$), and 5A (LTA) (Si/Al=1.0 and Na$^+$) were ion exchanged with Cu^{2+} at 80% ion exchanged to prepare 80CuNaY, 80CuNaMOR, and 80CuNa5A. 80CuNaY exhibited the highest electrical conductivity response under acetone and methanol exposures while 80CuNaMOR showed the highest response in n-heptane exposure which depended on the adsorption and solubility properties of each porous material. When adding dPPV into the 80CuNaY matrix, the minimum detection vapor concentration decreased in acetone, methanol, and n-heptane vapors. For the selectivity, the composite between 80CuNaY and dPPV responded only in the polar vapors (acetone, methanol) whereas dPPV_[90]80CuNaMOR responded only in the non polar vapor (n-heptane). The interactions between the sensing materials and the chemical vapors were investigated and identified by FTIR and AFM techniques.

Keywords: Gas Sensing Materials, Porous Materials, VOCs, Conducting Polymers, Composites

6.2 Introduction

Toxic gas and chemical vapor pollutions originated from the petroleum and petrochemical industries stimulate the concern for the development of gas sensors which using for detecting various kinds of toxic gas and vapor at low cost and with high sensitivity. Conducting polymers (Ruangchuay *et al.*, 2004; Jung *et al.*, 2008;

Benvenho *et al.*, 2009; Aguilar *et al.*, 2010; Kwon *et al.*, 2010; Ohira *et al.*, 2012; Hangarter *et al.*, 2013), porous materials (Vijaya *et al.*, 2008); and metal oxides (Vijaya *et al.*, 2008; Liu *et al.*, 2011) have been widely investigated for sensor applications.

Zeolites are one of the most important porous materials which are widely used in sensor technology, such as ZSM-5, L, beta, mordernite, and faujasites (zeolite X and Y). The advantages of zeolite are high porosity and surface area, good chemical stability, selectivity, and adsorption properties. Although these properties of zeolites have been utilized for sensing, there is the need to enhance the electrical conductivity and sensitivity towards a particular gas or vapor. The methods to improve the electrical conductivity response and sensitivity of a zeolite are through the ion exchanged process, dealumination of Si/Al ratio, and blending with high conducting materials. Blending with other conductive materials is one of factors to control the electrical conductivity value (Auerbach *et al.*, 2003; Tang *et al.*, 2008; Vijaya *et al.*, 2008; Chang *et al.*, 2011; Satsuma *et al.*, 2011; Varsani *et al.*, 2011; Hung *et al.*, 2012; Urbiztondo *et al.*, 2012).

The conducting polymers (CPs) like as poly(p-phenylene vinylene) (PPV), poly(pyrrole) (PPy), poly(aniline) (PANi), and poly(thiophene) (PTs) have high electrical conductivity responses when exposed to a toxic gas and vapor (Ruangchuay *et al.*, 2004; Jung *et al.*, 2008; Benvenho *et al.*, 2009; Aguilar *et al.*, 2010; Kwon *et al.*, 2010; Ohira *et al.*, 2012; Hangarter *et al.*, 2013). PPV is the one of conducting polymers which can be used in gas sensor application due to its high electrical conductivity response and sensitivity with good mechanical properties, chemical stability, and the ease to synthesize (Wessling *et al.*, 1968). The type of chemical vapors is the main factor which controls the positive and negative responses of doped poly(p-phenlene vinylene) or dPPV. The disadvantage of high conducting PPV is its poor selective properties. Therefore, previous work has combined the advantages of conducting polymers with good characteristics of zeolites to enhance the selective, adsorptive, and electrical properties toward gases and vapors (Wannatong *et al.*, 2008; Ayad *et al.*, 2009; Thongchai *et al.*, 2009; Arvand *et al.*, 2011; Chanthaanont *et al.*, 2012).

In this work, the effects of zeolite type and vapor concentration on the electrical conductivity response and sensitivity towards two different polar chemical vapors (acetone and methanol) and a nonpolar chemical vapor (n-heptane) were systematically investigated. Moreover, the composites between zeolite and dPPV were fabricated to study the effect of adding a conducting polymer on the responses towards the three chemical vapors. The FTIR and AFM techniques were used to investigate the interactions between the sensing materials and the chemical vapors.

6.3 Experimental

6.3.1 Sensing Materials Preparation

A conducting polymer poly(p-phenylene vinylene) or PPV was prepared following the Wessling route (Wessling *et al.*, 1968). The raw materials which were used to synthesize are α, α'-dichloro-p-xylene (Aldrich) and tetrahydro-thiophene (Aldrich). 18 M of sulfuric acid (H_2SO_4) was used as the doping agent. After the doping process, the bright yellow color of PPV was changed to black brown (Ahlskog *et al.*, 1997).

Zeolite Y (Si/Al=5.1 and Na^+) or NaY (Zeolyst), zeolite mordernite (Si/Al=18 and Na^+) or NaMOR (Tosoh Coperation, Japan), and zeolite 5A (LTA) (Si/Al=1.0 and Na^+) or Na5A (Sigma-Aldrich) were used in the 80% mole cation exchange. A 0.1 M solution of $CuCl_2$ was added into 5 grams of zeolite at 25 °C and stirred for 24 h to prepare zeolite Y (Si/Al=5.1, 20% mole of Na^+, and 80% mole of Cu^{2+}) or 80CuNaY, the zeolite mordernite (Si/Al=18, 20% mole of Na^+, and 80% mole of Cu^{2+}) or 80CuNaMOR, and the zeolite 5A (LTA) (Si/Al=1.0, 20% mole of Na^+, and 80% mole of Cu^{2+}) or 80CuNa5A. Then, the zeolite samples were filtered and washed with DI-water for 5 times (McKeen *et al.*, 2009; Chanthaanont *et al.*, 2012; Yimlamai *et al.*, 2011; Kamonsawas *et al.*, 2012; Kamonsawas *et al.*, 2013).

The composites were prepared by a physical mixing between the doped poly(p-phenylene vinylene) or dPPV into the zeolite matrices (80CuNaY, 80CuNaMOR, and 80CuNa5A) at the 10% v/v of dPPV. The sample pellets were formed by a hydraulic press at the pressure of 6 kN.

6.3.2 Characterization of Sensing Materials

The surface area and pore size of zeolite was investigated by surface area analyzer (Sorptomatic-1990). Spectra A300, Varian was used to determine the percentage of ion exchanged. A FT-IR spectrometer (Inclolet, model FRA 106/S) was used to characterize the functional groups of dPPV and to investigate the interactions between the chemical vapors and gas sensing materials. The morphology of gas sensing materials was investigated by a scanning electron microscope or SEM (Hitachi, TM 3000) at the magnifications of 10000x and 5000x and at 10 kV. An atomic force microscope or AFM (Park systems, XE-100) was used to characterize the phase changes during the chemical vapor exposure.

6.3.3 Electrical Conductivity Sensitivity Measurement

A voltage supplier (Keithley, 6517A) was connected with a custom made two point probes to measure the electrical conductivity of sensing materials under the air, N_2, and chemical vapor exposure where the voltage was varied and the resultant current was measured. The equation 6.1 was used to calculate the electrical conductivity value.

$$\sigma = (I/KVt) \qquad\qquad 6.1$$

where I is the measured current (A), V is the applied voltage (V), t is the thickness, and K is the geometric correction factor of the two-point probe which was determined by calibrating the probe with a silicon wafer possessing a known resistivity value.

The gas sensing experiment was measured by a flow system of gas detection unit which was connected with the custom made two point probes and the voltage supplier (Keithley, 6517A) to monitor the electrical conductivity change under the chemical vapor exposures. The chemical vapors in this paper were acetone, methanol, and n-heptane that were purchased from labscan (AR grade). The chemical vapor was generated by using nitrogen gas (N_2, TIG) at the concentrations of 30000 ppm (3% v/v), 3000 ppm (0.3% v/v), 300 ppm (0.03% v/v), 30 ppm (0.003% v/v), and 10 ppm (0.001% v/v). Equations 6.2 and 6.3 were used to calculate the electrical conductivity response and sensitivity of the gas sensing materials.

$$\Delta\sigma = \sigma_{\text{chemical vapor}} - \sigma_{\text{N2, before exposure}} \qquad 6.2$$

$$\text{Sensitivity} = \Delta\sigma / \sigma_{N_2 \text{ before exposure}} \qquad 6.3$$

where $\Delta\sigma$ is the difference in the specific electrical conductivity (S/cm), $\sigma_{\text{N2, before exposure}}$ is the specific electrical conductivity in N_2 before exposure (S/cm), and $\sigma_{\text{chemical vapor}}$ is the specific electrical conductivity under chemical vapor exposure (S/cm) (Kamonsawas *et al.*, 2012). The electrical conductivity in N_2 exposure was measured after air and moisture were evacuated from the chemical chamber when the electrical conductivity reached the steady state and recorded as $\sigma_{\text{N2, before exposure}}$. N_2 gas was evacuated and the chemical vapor was injected into the chamber. When the electrical conductivity reached a steady state, $\sigma_{\text{chemical vapor}}$ was recorded. Chemical vapor was removed by a vacuum pump and then N_2 gas was injected into the chamber and the electrical conductivity was measured and recorded as $\sigma_{\text{N2, after exposure}}$.

6.4 Results and Discussions

6.4.1 Characteristics of Zeolites and Composites

The main structures and analytical data of zeolites are listed in the Table 6.1. Zeolite Y (Si/Al=5.1 and Na^+) or NaY, zeolite mordenite (Si/Al=18 and Na^+) or NaMOR, and zeolite 5A (LTA) (Si/Al=1.0 and Na^+) or Na5A were ion exchanged with Cu^{2+} at the exchanged percentage of 80%. The ion exchanged percentage was measured by the atomic adsorption spectrophotometer (AAS) (Chanthaanont *et al.*, 2012). The ion exchanged percentages of 80CuNaY, 80CuNaMOR, and 80CuNa5A were 79%, 90%, and 80%, respectively.

Figure 6.1 shows the morphology of sensing materials. The morphology of dPPV, 80CuNaY, and 80CuNaMOR at the magnification of 10000x are shown in Figures 6.1b, 6.1c, and 6.1e, respectively. After mixing dPPV into 80CuNaY and 80CuNaMOR, the morphology of the composites are of nearly uniform dispersions as shown in Figures 6.1d and 6.1f.

Table 6.1 shows the electrical conductivity values of the zeolites under ambient condition. The electrical conductivity values of 80CuNaY, 80CuNaMOR, and 80CuNa5A are $5.48 \times 10^{-3} \pm 6.84 \times 10^{-4}$ S/cm, $1.89 \times 10^{-3} \pm 4.16$

$x10^{-5}$ S/cm, and 8.14 $x10^{-4}$ ± 4.27 $x10^{-7}$ S/cm, respectively. The electrical conductivity of zeolites depends on the ratio of silicon to aluminum (Si/Al ratio), the cation type, and the surface area. The high value of Si/Al ratio leads to an increase in the electrical conductivity in zeolites (McKeen *et al.*, 2009; Kamonsawas *et al.*, 2013). In this work, the zeolites have the same cations (Na^+ and Cu^{2+}). Although the Si/Al ratio of zeolite MOR (18) is higher than Y (5.1) and 5A (1.0), zeolite Y shows the highest electrical conductivity values relative to MOR and 5A, respectively. Because the high surface area presences the high amount of cation along the zeolite frame work leading to increase proton mobility and induce higher electrical conductivity. Therefore, 80CuNaY exhibited the highest electrical conductivity value.

6.4.2 The Temporal Response of Zeolites and Composites

The induction times (T_i) and recovery times (T_r) of the zeolites and their composites are shown in Table 6.2. In acetone exposure at the vapor concentration of 30000 ppm and 25 °C, the induction times of 80CuNaY, 80CuNaMOR, and 80CuNa5A are 42 ± 2, 35 ± 2, and 30 ± 2, respectively and the recovery times are 30 ± 2, 22 ± 1, and 20 ± 1 min, respectively. Generally, the cation type and surface area are expected to have effects on the induction and recovery times (Yimlamai *et al.*, 2011; Kamonsawas *et al.*, 2012; Kamonsawas *et al.*, 2013). The surface areas of 80CuNaY, 80CuNaMOR, and 80CuNa5A are 526 ± 2, 350 ± 15, and 283 ± 15 m^2/g, respectively. 80CuNaY shows the highest induction time and recovery time under the acetone exposure in comparison with 80CuNaMOR and 80CuNa5A due to the high surface area of zeolite Y.

For the effect of chemical vapor type, the induction times of 80CuNaY when exposed to acetone, methanol, and n-heptane at the vapor concentration of 30000 ppm, 25 °C are 40 ± 2, 45 ± 1, and 30 ± 2 min, respectively. The corresponding recovery times are 30 ± 2, 28 ± 0.2, and 20 ± 1.0 min, respectively. The induction and recovery times depend on the size of chemical vapor molecule. The small chemical vapor molecule size allows it to penetrate into the framework of zeolite easier than a larger molecule. The size of methanol is smaller than acetone and n-heptane. Thus, 80CuNaY takes the longer time to reach the

steady state in the methanol vapor exposure when compare with the acetone and n-heptane vapor. Other zeolite types and chemical vapor concentrations show similar behaviors (Ruangchuay *et al.*, 2004; Wannatong *et al.*, 2008; Yimlamai *et al.*, 2011; Kamonsawas *et al.*, 2012; Kamonsawas *et al.*, 2013; Yang *et al.*, 2011).

The effect of mixing 10% v/v of dPPV into the zeolites matrices and then exposed to acetone, methanol, and n-heptane vapors at the concentration of 30000 ppm, 25 °C and 1 atm is investigated next. The induction times of dPPV_[90]80CuNaY when exposed to acetone and methanol are 34 ± 2 and 36 ± 1, respectively. The recovery times are 24 ± 2 and 26 ± 1, respectively. The induction time of dPPV_[90]80CuNaMOR when exposed to n-heptane is 25 ± 0.5 and the recovery time is 15 ± 1.0, as shown in Table 6.2. The mixing of dPPV into all types of zeolites matrix thus reduces the induction time and recovery time due to the available active sites of dPPV (Yimlamai *et al.*, 2011; Kamonsawas *et al.*, 2012; Kamonsawas *et al.*, 2013).

6.4.3 The Electrical Conductivity Response of Zeolites and Composites
6.4.3.1 Effect of Zeolite Types and Chemical Vapors
Figure 6.2 and Table 6.3 show the electrical conductivity response and sensitivity of 80CuNaY, 80CuNaMOR, and 80CuNa5A. 80CuNaY, 80CuNaMOR, and 80CuNa5A under the effects of zeolite types towards two different of polar vapor (acetone and methanol) and a nonpolar vapor: n-heptane vapor at the vapor concentrations of 30000, 3000, 300, 30, and 10 ppm.

The electrical conductivity response of 80CuNaY, 80CuNaMOR, and 80CuNa5A during acetone exposure at the vapor concentration of 30000 ppm are $6.42 \times 10^{-04} \pm 2.02 \times 10^{-05}$, $2.60 \times 10^{-04} \pm 8.44 \times 10^{-04}$, and $2.48 \times 10^{-05} \pm 4.35 \times 10^{-06}$ S/cm, respectively. The corresponding electrical conductivity sensitivities are $4.87 \times 10^{-01} \pm 2.16 \times 10^{-02}$, $1.71 \times 10^{-01} \pm 3.06 \times 10^{-03}$, and $1.24 \times 10^{-01} \pm 1.95 \times 10^{-02}$, respectively as shown in Figure 6.2a and Table 6.3. The electrical conductivity response and sensitivity of zeolites thus depend on the zeolite type having different Si/Al ratios, cation types, and surface areas. In this work, the zeolites of the same cations (Na^+ and Cu^{2+}), the electrical conductivity response and sensitivity increase with increasing surface area. 80CuNaY exhibits the highest electrical conductivity

response and sensitivity towards acetone vapor due to the larger surface area of 80CuNaY (526 ± 2 m^2/g) when compared with 80CuNaMOR (350 ± 15 m^2/g) and 80CuNa5A (283 ± 15 m^2/g) (Thuwachaosoan *et al.*, 2007; Yimlamai *et al.*, 2011; Kamonsawas *et al.*, 2012; Kamonsawas *et al.*, 2013). Moreover, the Si/Al ratio has an effect on the electrical conductivity response and sensitivity. The low value of Si/Al ratio zeolite is more likely to adsorb the polar solvents such as acetone and methanol. The Si/Al ratio values of zeolites MOR, Y, and 5A are 18, 5.1, and 1.0, respectively. In this work, although 80CuNaY has the higher Si/Al ratio than 80CuNa5A, 80CuNaY has a larger surface area than 80CuNa5A. Therefore, 80CuNaY shows the highest response in acetone exposure whereas 80CuNa5A exhibits the lowest value.

For the other polar chemical vapors: methanol, the electrical conductivity responses of 80CuNaY, 80CuNaMOR, and 80CuNa5A in a methanol exposure at the vapor concentration of 30000 ppm are 6.57 x10^{-04} ± 4.03 x10^{-05}, 3.03 x10^{-04} ± 5.27 x10^{-06}, and 1.71 x10^{-04} ± 6.58 x10^{-06} S/cm, respectively. The corresponding electrical conductivity sensitivities are 7.90 x10^{-01} ± 2.15 x10^{-02}, 2.10 x10^{-01} ± 1.77 x10^{-01}, and 1.83 x10^{-01} ± 2.41 x10^{-04}, respectively as shown in Figure 6.2b and Table 6.3. The behavior of methanol exposure is similar to acetone exposure. With increasing surface area, the electrical conductivity response and sensitivity tend to increase. However, 80CuNaY, 80CuNaMOR, and 80CuNa5A show higher electrical conductivity response and sensitivity values in methanol exposure than in acetone exposure due to the size of chemical vapor. The small solvent molecule size allows it to penetrate into the zeolites framework and the size of methanol is smaller than acetone (Wannatong *et al.*, 2008; Thuwachaosoan *et al.*, 2007; Yimlamai *et al.*, 2011; Kamonsawas *et al.*, 2012; Kamonsawas *et al.*, 2013). Thus, all zeolites show significantly higher responses in methanol than acetone vapor.

Figure 6.2c and Table 6.3 show the electrical conductivity response and sensitivity towards a nonpolar vapor: n-heptane. The electrical conductivity response of 80CuNaY, 80CuNaMOR, and 80CuNa5A in n-heptane exposure at the vapor concentration of 30000 ppm are -5.38 x10^{-05} ± 4.17 x10^{-06}, -2.96 x10^{-04} ± 2.22 x10^{-04}, and -3.16 x10^{-05} ± 7.06 x10^{-06} S/cm, respectively. The

corresponding electrical conductivity sensitivities are -9.31 $\times 10^{-02}$ ± 3.06 $\times 10^{-03}$, -1.35 $\times 10^{-01}$ ± 2.93 $\times 10^{-02}$, and -8.78 $\times 10^{-02}$ ± 2.25 $\times 10^{-03}$, respectively. In case of nonpolar vapor, the high value of Si/Al ratio provides the hydrophobicity and capability to adsorb a nonpolar molecule than a polar molecule. 80CuNaMOR (Si/Al=18) has a higher Si/Al ratio than 80CuNaY (Si/Al=5.1) and 80CuNaA (Si/Al=1.0) (Yang *et al.*, 2007; Li *et al.*, 2010; Satsuma *et al.*, 2011; Ji *et al.*, 2012; Urbiztondo *et al.*, 2012). Thus, 80CuNaMOR shows the highest response towards n-heptane when compared with 80CuNaY and 80CuNaA. In the next part, 80CuNaY and 80CuNaMOR are further used to investigate the effect of dPPV.

6.4.3.2 Effect of dPPV and Chemical Vapor

Figure 6.3 shows the plot between the electrical conductivity response vs. vapor concentration (ppm) of dPPV_[90]80CuNaY and dPPV_[90]80CuNaMOR under acetone, methanol, and n-heptane at 25 °C, 1 atm, and at the vapor concentrations of 30000, 3000, 300, 30, and 10 ppm.

dPPV is mixed into the 80CuNaY matrix and the responses towards acetone and methanol at the vapor concentration of 30000 ppm were measured. The electrical conductivity response of dPPV_[90]80CuNaY towards acetone and methanol are 1.19 $\times 10^{-01}$ ± 7.44 $\times 10^{-03}$ and 2.11 $\times$ 10^{-01} ± 6.32 $\times 10^{-03}$ S/cm, respectively. The corresponding electrical conductivity sensitivity are 4.98 ± 6.96 $\times 10^{-02}$ and 5.77 ± 2.41 $\times 10^{-01}$, respectively as shown in Figure 6.3 and tabulated in Table 6.3. After mixing dPPV into the zeolite matrix, the electrical conductivity sensitivity increases by an order magnitude for all types of chemical vapor. This is because dPPV has the conjugated double bonds along the polymer chain leading to more electrons are able to transfer along the polymer chain, resulting in the higher values of the electrical conductivity response and sensitivity than that of the pristine 80CuNaY (Thuwachaosoan *et al.*, 2007; Wannatong *et al.*, 2008; Yimlamai *et al.*, 2011; Kamonsawas *et al.*, 2012; Kamonsawas *et al.*, 2013) as shown in Figure 6.4. For the electrical conductivity response and sensitivity towards n-heptane of dPPV_[90]80CuNaMOR are -1.57 $\times 10^{-03}$ ± 2.56 $\times 10^{-04}$ S/cm, and -3.64 $\times 10^{-01}$ ± 1.50 $\times 10^{-02}$, respectively. The results show that dPPV clearly enhances the response of 80CuNaMOR.

6.4.3.3 The Effect of Vapor Concentration

80CuNaY, 80CuNaMOR, and 80CuNa5A samples are investigated for the effect of vapor concentration where data are showed in Figure 6.2 and tabulated in Table 6.3. Figures 6.2a and 6.2b show the plot between electrical conductivity responses of zeolites vs. vapor concentration (ppm). In the case of polar solvents (acetone and methanol), the minimum vapor concentration which 80CuNaY could respond is 6 and 5 ppm, respectively. (Yang et al., 2007; Wannatong et al., 2008 Li et al., 2010; Ji et al., 2012; Urbiztondo et al., 2012). With decreasing vapor concentration, the electrical conductivity response and sensitivity of all samples generally decrease. In the case of nonpolar vapor (n-heptane), 80CuNaMOR could respond at the lowest vapor concentration of 6 ppm. The nonpolar vapor prefers to absorb a high Si/Al ratio value zeolite which posssesses the hydrophobicity. 80CuNaMOR (Si/Al=18) has a higher Si/Al ratio than 80CuNaY (Si/Al=5.1) and 80CuNa5A (Si/Al=1.0). Therefore, 80CuNaMOR exhibits the highest responses in n-heptane and the lowest minimum vapor concentrations as shown in Figures 6.2c and 6.4 and data tabulated in Table 6.3.

When mixing dPPV into the zeolite matrices at the ratio of dPPV of 10% v/v, dPPV improves the electrical conductivity response of zeolites. In the polar vapors (acetone and methanol), the minimum vapor concentration of dPPV_[90]80CuNaY in acetone vapor decreases from 9 ppm to 4 ppm and in methanol vapor is reduced from 5 ppm to 2 ppm as shown in Figure 6.3, 6.4 and tabulated in Table 6.3. For the non polar solvent n-heptane, the minimum vapor concentration of dPPV_[90]80CuNaMOR decreases from 6 ppm to 5 ppm (Yang et al., 2007; Wannatong et al., 2008 Li et al., 2010; Yimlamai et al., 2011; Ji et al., 2012; Urbiztondo et al., 2012).

The three different chemical vapors possess different degrees of hydrophilicity. The low Si/Al ratio zeolite (80CuNaY) is more likely to adsorb the polar vapors (acetone and methanol) due to its hydrophilic properties and exhibits the positive response (Yang et al., 2007; Wannatong et al., 2008 Li et al., 2010; Satsuma et al., 2011; Ji et al., 2012; Urbiztondo et al., 2012). After mixing dPPV into the zeolites matrix, the electrical conductivity sensitivities towards acetone and methanol increase by an order magnitude as shown in Figure 6.4. For the high ratio of Si/Al

ratio zeolite (80CuNaMOR) with the high hydrophobic properties, it responds in the nonpolar vapor (n-heptane) better than in the polar vapor (Satsuma *et al.*, 2011; Urbiztondo *et al.*, 2012). In summary, dPPV can enhance the electrical conductivity responses of the zeolites for all chemical vapors examined.

In the previous work (Kamonsawas *et al.*, 2012; Kamonsawas *et al.*, 2013), NaY is ion exchanged with Cu^{2+} and blended with dPPV showed the greatest response towards two polar vapors (ketone and methanol) when compared with other cations (K^+, Mg^{2+}, Ca^{2+}, Ni^{2+}, and Fe^{2+}). In this work, dPPV_[90]80CuNaY did not respond at all in the non polar vapor (n-heptane) due to the solubility properties between 80CuNaY and the chemical vapor. To compare with other materials, zeolite 4A, 5A, X, and Y were used to study the effect of four different chemical vapors (methanol, acetone, and hexane). The results suggested that zeolite 5A had a suitable pore size and solubility properties to adsorb n-hexane and exhibited the highest response to n-hexane (Yang *et al.*, 2007). Thus, it was confirmed that after mixing various types of zeolite into a conductive polymer, the selective properties were significantly improved.

6.4.4 Investigations of the Reactions of Adsorbed Chemical Vapor

6.4.4.1 FTIR Technique

The interaction of gas sensing materials with acetone, methanol and n-heptane vapor was investigated by the FTIR technique. The FTIR spectra of gas sensing materials were taken in the 650-4000 cm^{-1} region.

The FTIR spectra of dPPV_[90]80CuNaY before, during, and after acetone exposure are shown in Figure 6.5. The adsorption peaks at 1150, 1514, and 3012 cm^{-1} indicate the characteristic peaks of dPPV (Thongchai *et al.*, 2009; Kamonsawas *et al.*, 2010; Kamonsawas *et al.*, 2012; Kamonsawas *et al.*, 2013. The characteristic peak of zeolite Y is at 3650 cm^{-1} (Thuwachaosoan *et al.*, 2007; Yimlamai *et al.*, 2011). The new peaks at 3449 and 1210 cm^{-1} during acetone exposure are suggested to be an interaction between acetone and zeolite Y (Biaglow *et al.*, 1993; Florian *et al.*, 1994; Thuwachaosoan *et al.*, 2007; Yimlamai *et al.*, 2011). The new peak at 1377 cm^{-1} is due to the C-O interaction between acetone and dPPV, as shown in Figure 6.8a. The intensity of peak at 1150 cm^{-1} increases because

of the increase in the quinoid structures along dPPV structure (Thongchai *et al.*, 2009; Kamonsawas *et al.*, 2010; Kamonsawas *et al.*, 2012; Kamonsawas *et al.*, 2013). After evacuating the system, the intensities of the peaks at 1514 and 3012 cm^{-1} decreases since the acetone molecule acted as a secondary dopant leading to increase the number of the quinoid structures along the dPPV chain (Thongchai *et al.*, 2009; Kamonsawas *et al.*, 2010; Kamonsawas *et al.*, 2012; Kamonsawas *et al.*, 2013). The interaction was clearly irreversible.

Figure 6.6 shows the FTIR spectrum of dPPV_[90]80CuNaY before, during, and after methanol exposure. Before the methanol exposure, the peaks are at the same wavenumbers as in Figure 6.5. During the methanol exposure, three new peaks at 2971, 2875, and 1053 cm^{-1} occur due to the interaction between the OH group of methanol and zeolite Y (Thongchai *et al.*, 2009; Kamonsawas *et al.*, 2010; Kamonsawas *et al.*, 2012; Kamonsawas *et al.*, 2013). Another new peak at 1354 cm^{-1} represents the interaction of C-O between methanol and dPPV, as shown in Figure 6.8b. The intensity of peak at 1150 cm^{-1} increases due to the increase of the quinoid structures on dPPV chain (Thongchai *et al.*, 2009; Kamonsawas *et al.*, 2010; Kamonsawas *et al.*, 2012; Kamonsawas *et al.*, 2013). After methanol exposure, these peaks still remain and this interaction is thus irreversible.

Figure 6.7 shows the FTIR spectrum of dPPV_[90] 80CuNaMOR before, during, and after n-heptane exposure. Before n-heptane exposure, the adsorption peaks at 1140, 1510, and 3018 cm^{-1} appear as the characteristic peaks of dPPV (Thongchai *et al.*, 2009; Kamonsawas *et al.*, 2010; Kamonsawas *et al.*, 2012; Kamonsawas *et al.*, 2013). The characteristic peak of zeolite mordernite is at 3667 cm^{-1} and can be assigned as the Si-OH group. The peaks at 1080 and 1230 cm^{-1} are characteristic peaks of the SiO$_4$ unit (Biaglow *et al.*, 1993; Florian *et al.*, 1994; Hoost *et al.*, 1996; Panov *et al.*, 1998; Thuwachaosoan *et al.*, 2007; Martin *et al.*, 2008; Yang *et al.*, 2007; Yimlamai *et al.*, 2011). During n-heptane exposure, three new peaks at 1416, 2875, and 2927 cm^{-1} appear due to the C-H stretching between n-heptane and dPPV. The three new peaks at 1416, 2875, and 2927 cm^{-1} represent the interaction between n-heptane and zeolite mordenite as shown the mechanism in Figure 6.8c (Biaglow *et al.*, 1993; Florian *et al.*, 1994; Hoost *et al.*, 1996; Panov *et al.*, 1998; Thuwachaosoan *et al.*, 2007; Martin *et al.*,

2008; Yang *et al.*, 2007; Yimlamai *et al.*, 2011). After n-heptane exposure, these peaks still remain and this interaction is thus irreversible.

The interactions of dPPV_[90]80CuNaY with acetone and methanol vapor are shown in Figures 6.8a and 6.8b. The interaction between acetone and dPPV_[90]80CuNaY occurred via the electron transfer from acetone to the copper cation in the 80CuNaY. For the dPPV structure, the lone pair electron on the carbonyl group of the acetone molecule stabilizes the cation along the dPPV chain resulting in greater negative charges corresponding to higher electrical conductivity when exposed to the acetone vapor (Thongchai *et al.*, 2009; Kamonsawas *et al.*, 2010; Kamonsawas *et al.*, 2012; Kamonsawas *et al.*, 2013). In case of methanol, the interaction between dPPV_[90]80CuNaY and methanol is initiated by the electron transfer from oxygen on the OH group to copper cation in the zeolite Y structure leading to the cation mobility along the zeolite framework and an increase in the electrical conductivity. For the interaction between dPPV and methanol, the lone pair electron on the methanol molecule stabilizes the cation on the dPPV chain and resulting in higher electrical conductivity during methanol exposure (Biaglow *et al.*, 1993; Florian *et al.*, 1994; Hoost *et al.*, 1996; Panov *et al.*, 1998; Thuwachaosoan *et al.*, 2007; Martin *et al.*, 2008; Yang *et al.*, 2007; Thongchai *et al.*, 2009; Kamonsawas *et al.*, 2010; Yimlamai *et al.*, 2011; Kamonsawas *et al.*, 2012; Kamonsawas *et al.*, 2013). Figure 6.8c shows the interaction between dPPV_[90]80CuNaMOR and n-heptane. The interaction starts with the oxygen on the zeolite mordernite and H on n-heptane. For the dPPV chain, the anion on the dPPV chain donates the electron to the H atom on n-heptane resulting in higher electrical conductivity (Biaglow *et al.*, 1993; Florian *et al.*, 1994; Hoost *et al.*, 1996; Panov *et al.*, 1998; Thuwachaosoan *et al.*, 2007; Yang *et al.*, 2007; Martin *et al.*, 2008; Thongchai *et al.*, 2009; Kamonsawas *et al.*, 2010; Yimlamai *et al.*, 2011; Kamonsawas *et al.*, 2012; Kamonsawas *et al.*, 2013).

6.4.4.2 AFM Technique

The EFM mode is used to investigate the interaction between the sensing materials and chemical vapors under applied voltage at the tip of -8V. Figure 6.9 shows the phase images of dPPV_[90]80CuNaY before and after

methanol exposure, respectively and the plot between charged generated vs. distance.

The dPPV_[90]80CuNaY shows the positive charge methanol exposures under applied a negative voltage at the tip; the bright areas appear due to the attractive force between the tip and dPPV_[90]80CuNaY as shown in Figure 6.9a. After methanol exposure, the sample shows the dark area due to the repulsive force between the tip and the active sites of 80CuNaY as shown in Figure 6.9b. For the acetone vapor, the phased image changes similarly to the methanol vapor. In case of dPPV_[90]80CuNaY exposure to the acetone vapor and dPPV_[90]80CuNaMOR in the n-heptane vapor, the phased images change from bright areas to dark areas when exposed to n-heptane similar to the dPPV_[90]80CuNaY sample. Figure 6.9c shows the plot between degree of charge generated vs. sample distance before and after the acetone and methanol exposures. The plot shows the phase image changes from bright areas to dark areas and the degree of charges generated changes from -17.12 to -23.90 in the methanol exposure. Thus, it can be concluded that the interaction between dPPV_zeolite Y and the chemical vapor clearly induced the phase changes under the chemical vapor exposures.

6.5 Conclusions

Three different types of zeolite: zeolite Y (Si/Al=5.1 and Na^+), mordenite (Si/Al=18 and Na^+) and 5A (LTA) (Si/Al=1.0 and Na^+) were used in the ion exchanged process with 0.1 M of $CuCl_2$ to prepare 80% mole cation exchange of 80CuNaY, 80CuNaMOR, and 80CuNa5A. The modified zeolites were studied for the selective properties towards three different chemical vapors (acetone, methanol, and n-heptane). The highest electrical conductivity response and sensitivity when exposed to acetone and methanol vapor at the vapor concentration of 30000 ppm was obtained from 80CuNaY while 80CuNaMOR showed the highest electrical conductivity response and sensitivity in n-heptane vapor due to the adsorption and solubility properties in each material. 80CuNa5A exhibited the lowest values when exposed to the three different chemical vapors due to the low surface area. In order to

study the effect of dPPV and chemical vapor concentration, dPPV was mixed into 80CuNaY and 80CuNaMOR at 10% v/v dPPV and exposed to acetone, methanol, and n-heptane. When mixing dPPV into the 80CuNaY matrix, the minimum vapor concentration towards in acetone vapor decreased from 7 to 4 ppm and in methanol vapor decreased from 5 to 2 ppm. dPPV_[90]80CuNaMOR responded well to n-heptane at the vapor concentration of 5 ppm which was reduced from 6 ppm for the 80CuNaMOR. It can be concluded that adding dPPV definitely improved the electrical conductivity response and sensitivity toward the three different chemical vapors (acetone, methanol, and n-heptane). The interaction between gas sensing materials and the chemical vapors were identified by FTIR and AFM techniques and shown to be irreversible.

6.6 Acknowledgements

6.7 References

Ahlskog, M., Reghu.M., Noguchi, T., and Ohnishi, T. (1997) Doping and conductivity studies poly(p-phenylene vinylene). Synthetic Metals, 89, 11-15.

Aguilar, A.D., Forzani. E.S., Leright, M., Tsow, F., Cagan, A., Iglesias, R.A., Nagahara, L.A., Amlani, I., Tsiu, R., and Tao, N.J. (2010) A hybrid nanosensor for TNT vapor detection. Nano Letters, 10, 380-384.

Arvand, M., Ansari, R., and Heydari, L. (2011) Development of a conductive composite based on polythiophene/Y-zeolite and its response towards sulfide ions. Materials Science and Engineering: C, 31, 1398-1404.

Auerbach, S.M., Carrado, K.A., and Dutta, P.K. (Eds.) (2003) Handbook of Zeolite Science and Technology. New York: Marcel Dekker.

Ayad, M.M., Hefnawey, G.El., and Torad, N.L. (2009) A sensor of alcohol vapours based on thin polyaniline base film and quartz crystal microbalance. Journal of Hazardous Materials. 168, 85-88.

Benvenho, A.R.V., Li, R.W.C., and Gruber, J. (2009) Polymeric electronic gas sensor for determining alcohol content in automotive fuels. Sensor and Actuators B: Chemical, 136, 173-176.

Biaglow, A.I., Gorte, R.J., and David W. (1993) Molecular motions and 13C chemical shift anisotropy of acetone adsorbed inH-ZSM-5 zeolite. Journal of Physical Chemistry B. 97, 7135-713.

Chang, J.C., Hung, S.T., Lin, C.K., Chen, C.Y., and Kuo, E.H. (2010) Selective growth of ZnO nanorods for gas sensors using ink-jet printing and hydrothermal processes. Thin Solid Films, 519, 1693-1698.

Chanthaanont, P. and Sirivat, A. (2012) Interaction of carbon monoxide with PEDOT-PSS/zeolite composite: effect of Si/Al ratio of ZSM-5 zeolite. e-Polymer. 12(1), 106-116.

Florian, J. and Kubelkova, L. (1994) Proton transfer between H-zeolite and adsorbed acetone or acetonitrile: quantum chemical and FTIR study. Journal of Physical Chemistry C. 98, 8734-8741.

Hangarter, C.M., Chartuprayoon, N., Hernandez, S.C., Choa, Y., and Myung, N.V. (2013) Hybridized conducting polymer chemiresistive nano-sensors. Nanotoday, 291, 1-17.

Hoost, T.E., Laframboise, K.A., and Otto, K. (1996) Infrared study of acetone and nitrogen oxides on Cu-ZSM-5. Catalysis Letters. 37, 153-156.

Hung, S.T., Chang, C.J., Hsu, C.H., Chu, B.H., Lo, C.F., Hsu, C.C., Pearton, S.J., and Holzworth, M.R. (2012) SnO_2 functionalized AlGaN/GaN high electron mobility transistor for hydrogen sensing application. International Journal of Hydrogen Energy. 37. 13783-13788.

Ji, X., Yao, W., Peng, J., Ren, N., Zhou, J., and Huang, Y. (2012) Evaluation of Cu-ZSM-5 zeolites as QCM sensor coatings for DMMP detection. Sensors and Actuators B: Chemical, 166-167, 50-55.

Jung, Y.S., Jung, W., Tuller, H.L., and Ross, C.A. (2008) Nanowire conductive polymer gas sensor patterned using self-assembled block copolymer lithography. Nano Letters. 8, 3776-3780.

Kamonsawas, J., Sirivat, A., Niamlang, S., Hormnirun, P., and Prissanaroon-Ouijai, W. (2010) Electrical conductivity response of poly(phenylene vinylene)/ zeolite composites exposed to ammonium nitrate. Sensors, 10, 5590-5603.

Kamonsawas, J., Sirivat, A., and Hormnirun, P. (2012) Poly(phenylene vinylene)/ zeolite Y composite as a ketone vapors sensor: effect of alkaline cations. Journal of Polymer Research, 19, 1-12.

Kamonsawas, J., Sirivat, A., and Hormnirun, P. (2013) Sensitive and selective responses of poly(phenylene vinylene)/zeolite Y-based sensors towards ketone vapors. International Journal of Polymeric Materials and Polymeric Biomaterials, 62(11), 583-589.

Kwon, O.S., Hong, J.Y., Park, S.J., Jang, Y., and Jang, J. (2010) Resistive gas sensors based on precisely size-controlled polypyrrole nanoparticles: effects of particle size and deposition method. Journal of Physical Chemistry C. 114, 18874-18879.

Li, X. and Dutta, P.K. (2010) Interaction of dimethylmethylphosphate with zeolite Y: impedance-based sensor for detecting nerve agent simulants. Journal of Physical Chemistry C, 114. 7986-7994.

Liu, X., Cheng, S., Liu, H., Hu, S., Zhang, D., and Ning, H. (2012) A survey on gas sensing technology. Sensors, 12, 9635-9665.

Martins, A.V.G., Berlier, G., Bisio, C., Coluccia, S., Pastore, H.O., and Marchese, L. (2008) Quantification of bronsed sites in microporous catalysts by a combined FTIR and NH_3-TPD study. Journal of Physical Chemistry C, 112, 7139-7120.

McKeen, J.C. and Davis, M.E. (2009) Conductivity of mo-and divalent cation in the microporous zincosilicate VPI9. Journal of Physical Chemistry C, 113, 9870-9877.

Ohira, S.I., Goto, K., Toda, K., and Dasgupta, P.K. (2012) A capacitance sensor for water: trace moisture measurement in gases and organic solvents. Analytical Chemistry, 84, 8891-8897.

Panov, A.G. and Fripiat, J.J. (1998) An infared study of acetone and mesityl oxide adsorption on acid catalyst. Langmuir, 14, 3788-3796.

Ruangchuay, L., Sirivat, A., and Schwank, J. (2004) Selective conductivity response of polypyrrole-based sensor on flammable chemicals. Reactive and Functional Polymers, 61, 11-22.

Satsuma, A., Yang, D., and Shimizu, K.I. (2011) Effect of pore diameter of zeolites on detection of base molecules by zeolite thick film sensor. Microporous and Mesoporous Materials, 141, 20-25.

Tang, Li., Li, Y., Xu, K., Hou, X., and Lv, Y. (2008) Sensitive and selective acetone sensor based on its cataluminescence from Nano-La_2O_3 Surface. Sensors and Actuators B: Chemical, 132, 243-249.

Thongchai, N., Kunanuruksapong, R., Niamlang, S., Wannatong, L., Sirivat, A., and Wongkasemjit, S. (2009) Interactions between CO and poly(p-phenylene vinylene) as induced by ion-exchanged zeolites. Materials, 2, 2259-2275.

Thuwachaosoan, K., Chottananont, D., Sirivat, A., Rujiravanit, R., and Schwank, J. (2007) Electrical conductivity responses and interactions of poly(3-thiopheneacetic acid)/zeolites L, mordenite, beta, and H_2. Materials Science and Engineering: B, 140, 23-30.

Urbiztondo, M.A., Peralta, A., Pellejero, I., Sese, J., Pina M.P., Dufour, I., and Santamaria, J. (2012) Detection of organic vapours with Si cantilevers coated with inorganic (zeolite) or organic (polymer) layers. Sensors and Actuators B: Chemical, 171-172, 822-831.

Varsani, P., Afonja, A., Williams, D.E., Parkin, I.P., and Binions, R. (2011) Zeolite-modified WO_3 gas sensors-enhanced detection of NO_2. Sensors and Actuators B: Chemical, 160, 475-482.

Vijaya, J.J., Kenedy, L.J., Sekaran, G., Bayhan, M., and William, M. (2008) Preparation and VOC gas sensing properties of Sr(II)-added copper aluminate spinel composites. Sensors and Actuators B: Chemical, 134, 604-612.

Wannatong, L., Sirivat, A., and Schwank, J. (2008) Polypyrrole and its composites with 3A zeolite and polyamide 6 as sensors for four chemicals in lacquer thinner. Reactive and Functional Polymers, 68, 1646-1651.

Wessling, R.A., and Zimmerman, R.G. (1968) Polyelectrolytes from bis-sulfonium salts. U.S.Patent. 3, 401.

Yang. P., Ye, X., Lau, C., Li, Z., Liu, X., and Lu, J. (2007) Design of efficient zeolite sensor materials for n-hexane. Analytical Chemistry, 79, 1425-1432.

Yasada, K.E., Visser, J.H., and Bein, T. (2009) Molecular sieve catalysts on microcalorimeter chips for selective chemical sensor. Microporous and Mesoporous Materials, 119, 356-359.

Yimlamai, I., Niamlang, S., Chanthaanont, P., Kunanuruksapong, R., Changkhamchom, S., and Sirivat, A. (2011) Electrical conductivity response and sensitivity of ZSM-5, Y and mordenite zeolite towards ethanol vapor. Ionics, 17, 607-615.
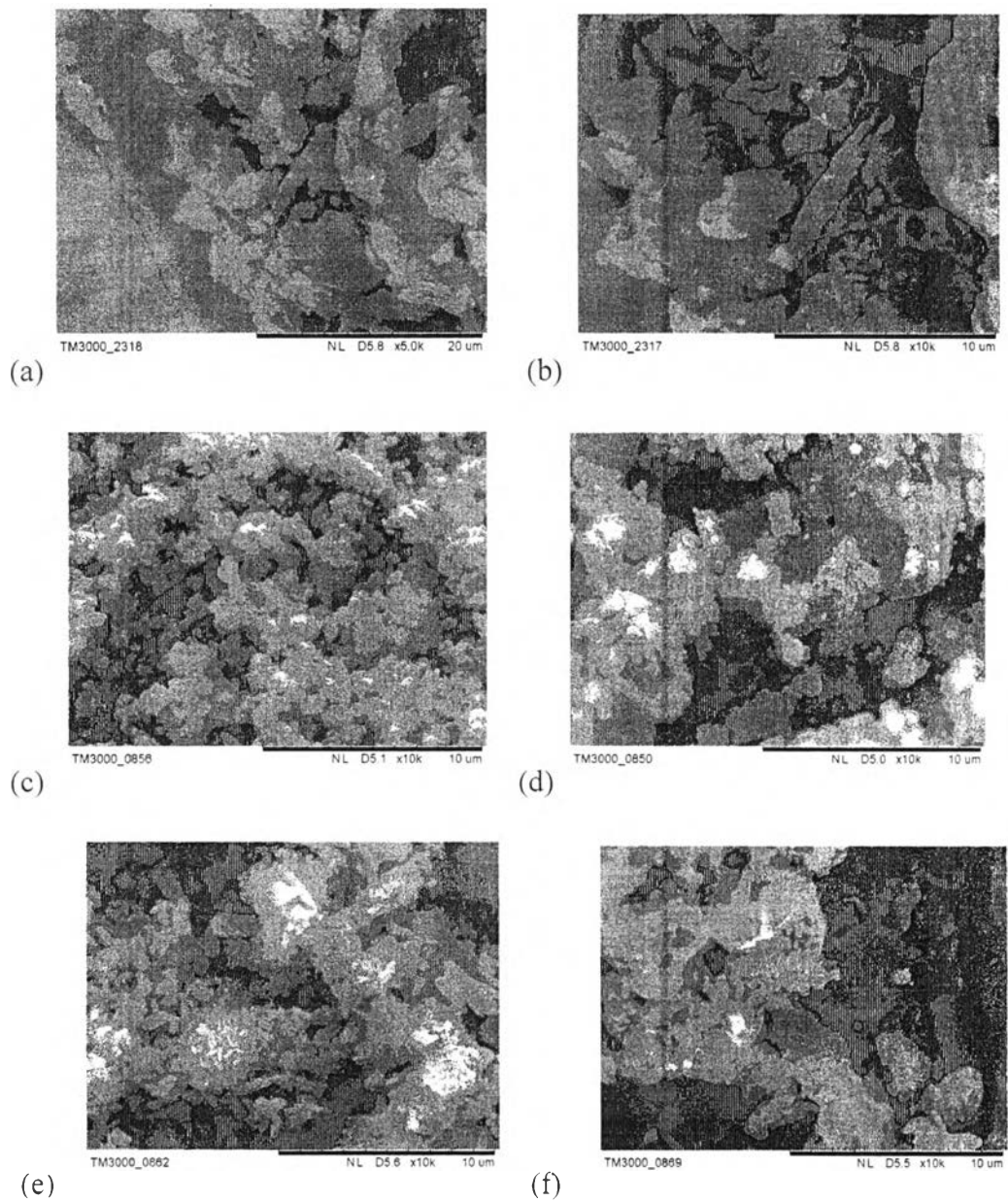
Figure 6.1 The morphology of dPPV, 80CuNaY powders , 80CuNaMOR powder, dPPV_[90]80CuNaY composites with 10% v/v of dPPV and dPPV_[90] 80CuNaMOR composites with 10% v/v of dPPV: (a) dPPV at magnification of 5000; (b) dPPV at magnification of 10000; (c) 80CuNaY at magnification 10000; (d) dPPV_[90]80CuNaY at magnification of 10000; (e) 80CuNaMOR at magnification 10000; and (f) dPPV_[90]80CuNaMOR at magnification of 10000.
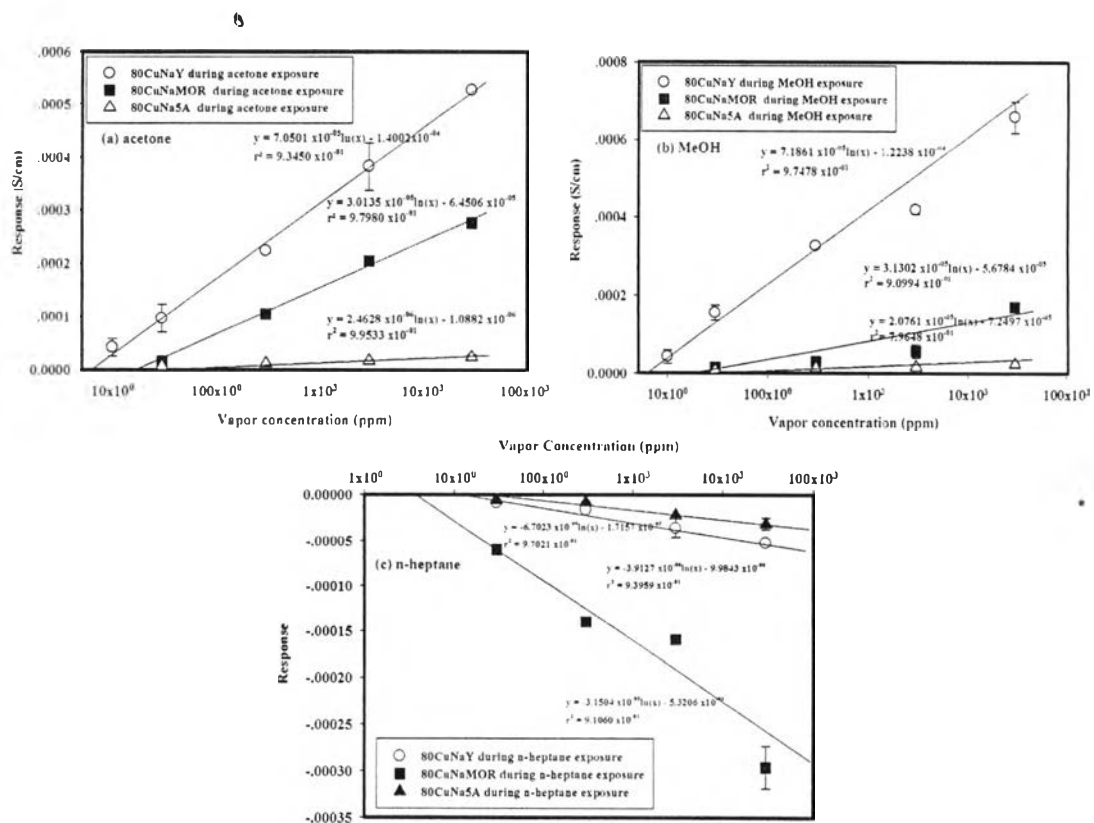
Figure 6.2 Electrical conductivity response of the NaY, 80CuNaY, 80CuNaMOR, and 80CuNa5A under: (a) acetone; (b) methanol; and (c) n-heptane exposures at 25 °C, 1 atm, and at vapor concentrations of 30000, 3000, 300, 30, and 10 ppm.
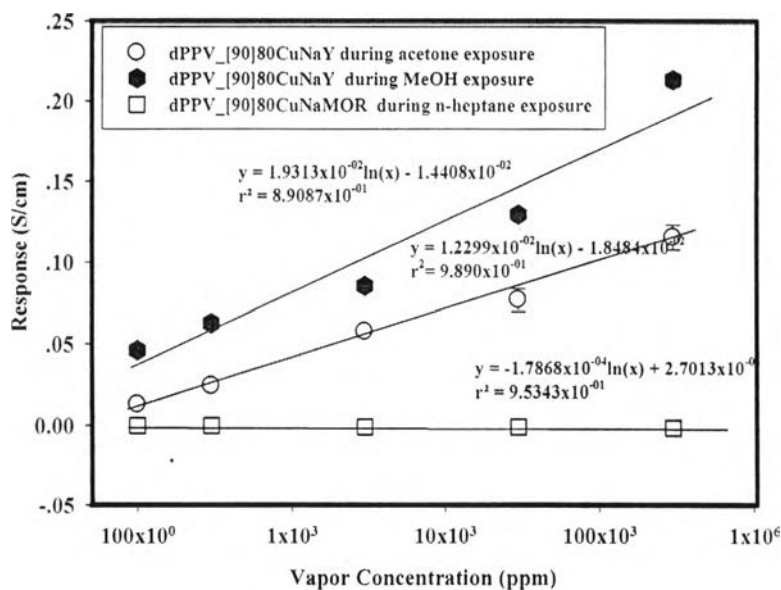
Figure 6.3 The electrical conductivity responses of dPPV_[90]80CuNaY to acetone and methanol exposures and dPPV_[90]80CuNaMOR to n-heptane exposure at 25 °C, 1 atm, and at vapor concentrations of 30000 ppm, 3000 ppm, 300 ppm, 30 ppm, and 10 ppm.
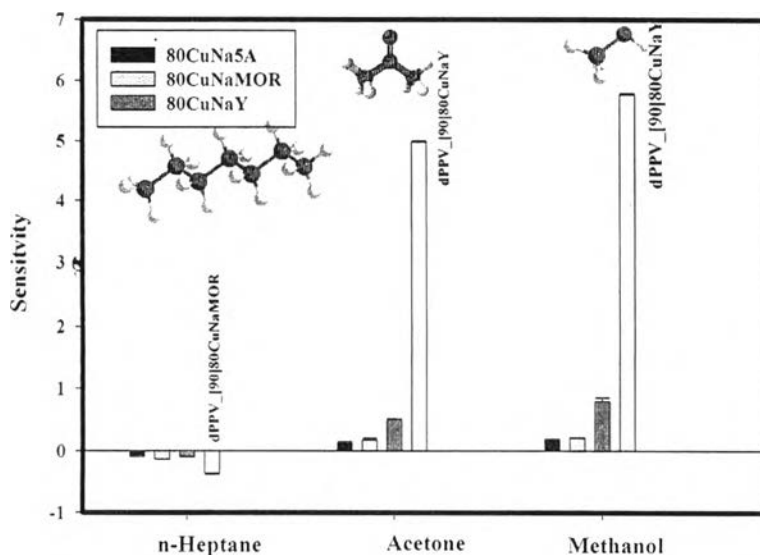
Figure 6.4 The electrical conductivity response of sensing materials to acetone, methanol, and n-heptane exposures at 25 °C, 1 atm, at vapor concentration of 30000 ppm.
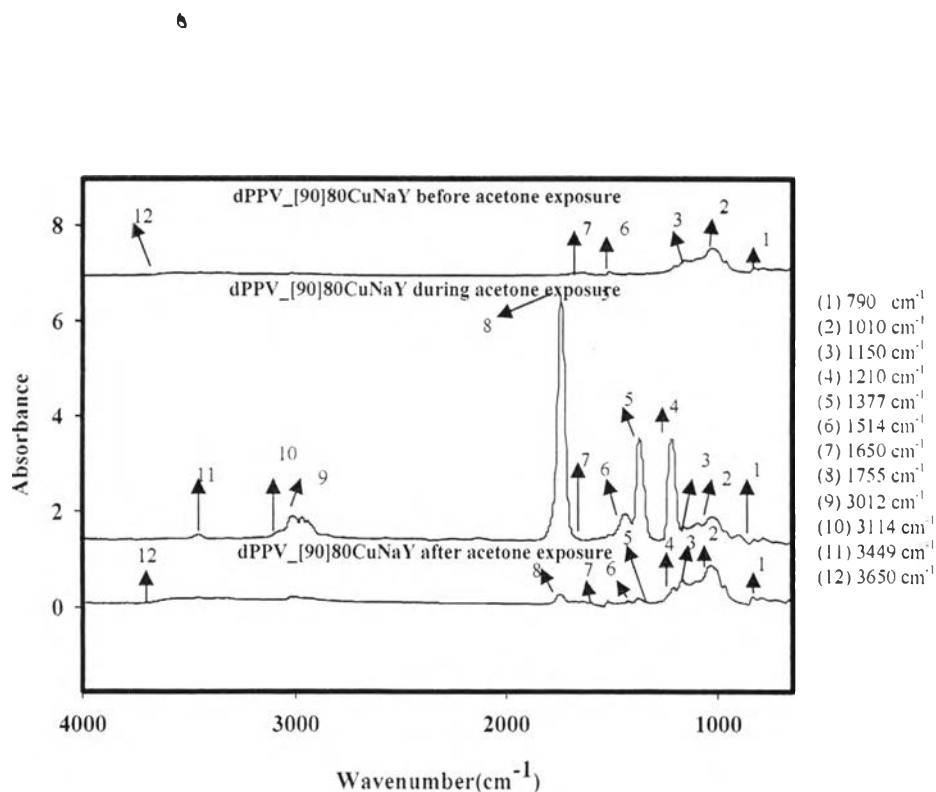
Figure 6.5 FTIR spectra of dPPV_[90]80CuNaY exposed to acetone at vapor concentration of 30000 ppm (pressure at 1 atm and at T=25 °C).
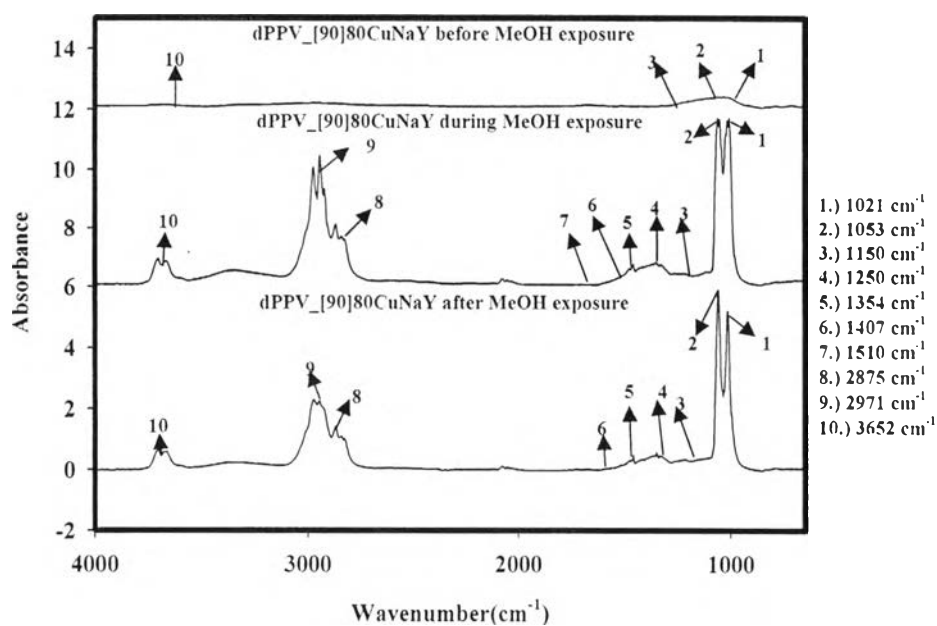
Figure 6.6 FTIR spectra of dPPV_[90]80CuNaY exposed to methanol at vapor concentration of 30000 ppm (pressure at 1 atm and at T=25 °C).
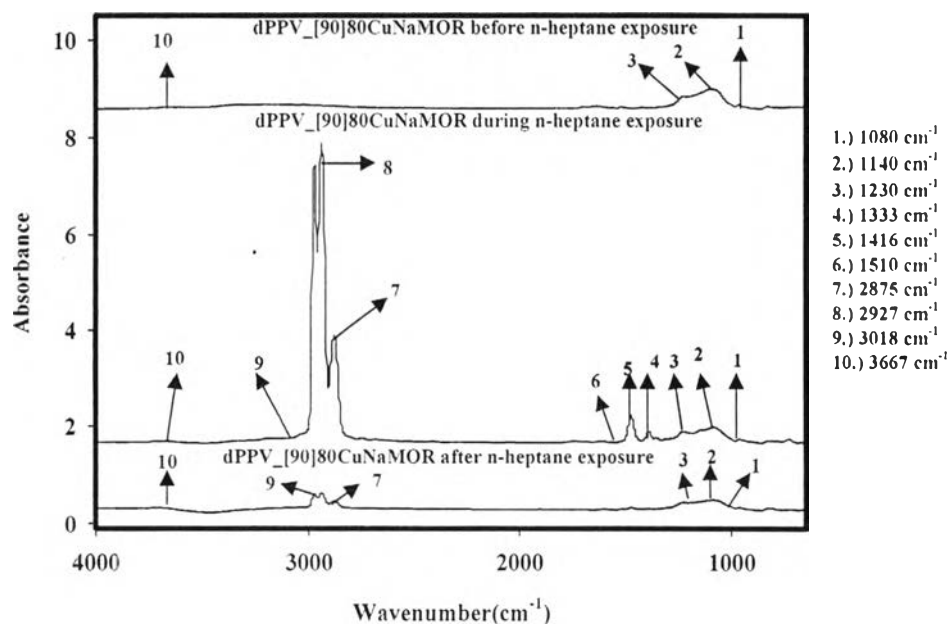
Figure 6.7 FTIR spectra of dPPV_[90]80CuNaMOR exposed to n-heptane at vapor concentration of 30000 ppm (pressure at 1 atm and at T=25 °C).

(a) acetone exposure
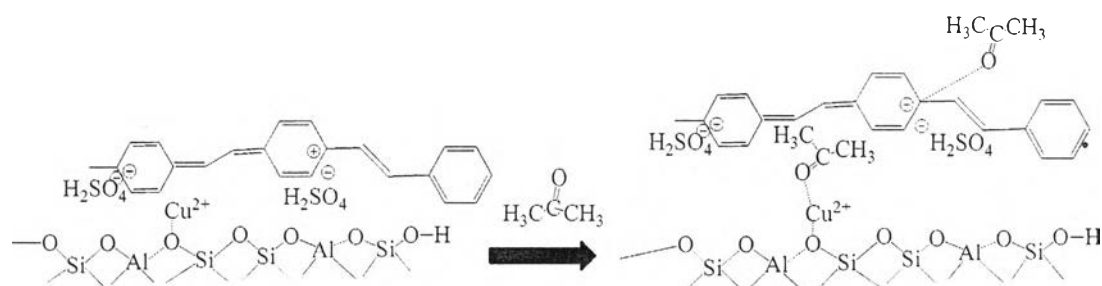
(b) methanol exposure
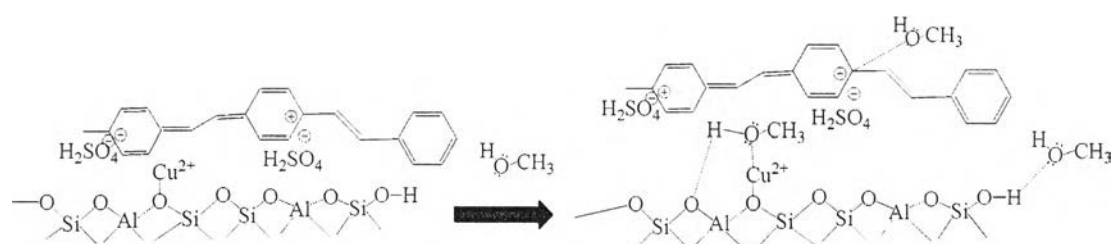
(c) n-heptane exposure
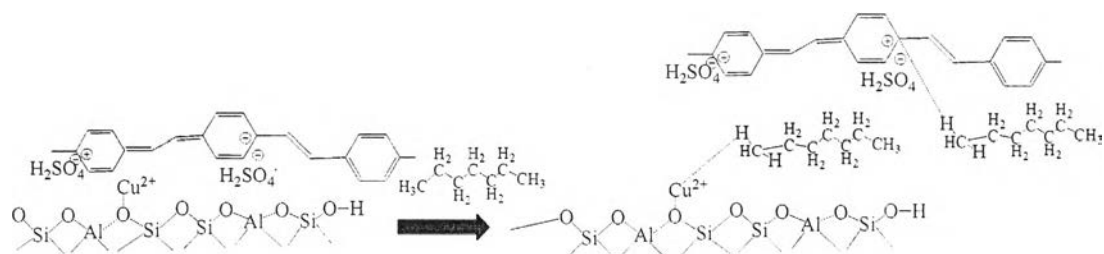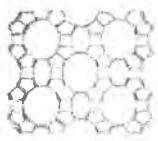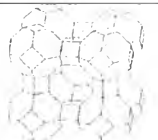
Figure 6.8 Mechanisms of the interactions between: (a) acetone vapor and dPPV_ [90]80CuNaY; (b) methanol vapor and dPPV_[90]80CuNaY; and (c) n-heptane vapor and dPPV_[90]80CuNaMOR.

Before Methanol Exposure   After Methanol Exposure

Phase

Image

(a) At 25 °C, Sample bias -8V   (b) At 25 °C, Sample bias -8V

(c)
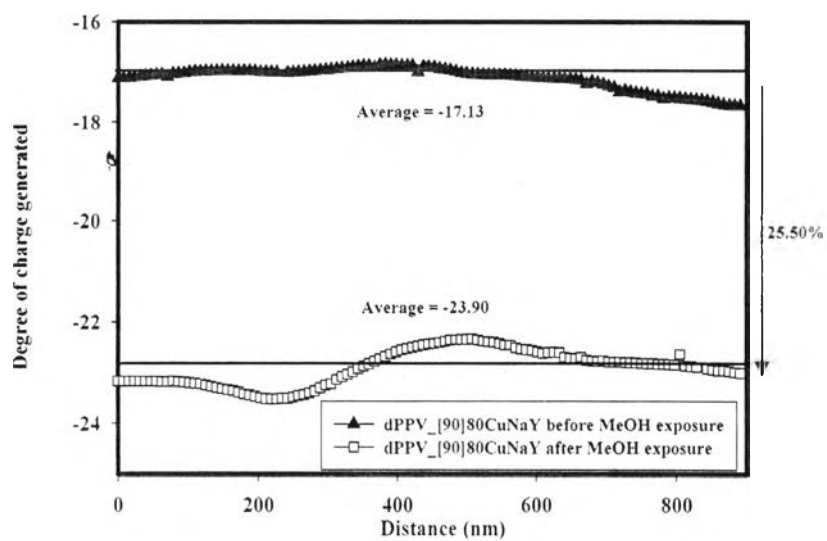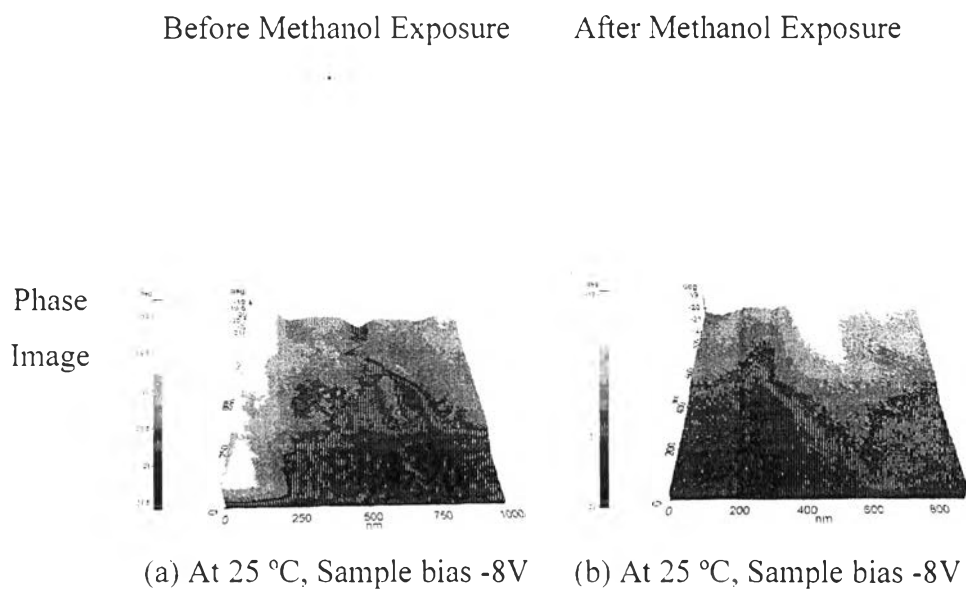
Figure 6.9 EFM-Phase images of: (a) dPPV_[90]80CuNaY before exposure; (b) during methanol exposure; and (c) degree of charges generated on dPPV_[90] 80CuNaY under -8 V of tip bias across the whole region.

Table 6.1 Analytical data and electrical conductivity of modified zeolites

Sample	Chemical Structure	Sample Code	% Mole of Cation	EN	Cationic Radii (Å)	Median Pore Width (Å)	Surface Area (m²/g)	σ_{air} (S/cm)
Zeolite Y (Si/Al=5.1, Na$^+$, and Cu^{2+})		80CuNaY	79% Cu^{2+} and 21% Na$^+$	0.93 (Na$^+$) and 1.372 (Cu^{2+})	1.16 (Na$^+$) and 0.87 (Cu^{2+})	7.092 ± 0.04	526.0 ± 2.0	5.48 x10^{-3} ± 6.48 x10^{-4}
Zeolite MOR (Si/Al=18, Na$^+$, and Cu^{2+})		80CuNaMOR	90% Cu^{2+} and 10% Na$^+$	0.93 (Na$^+$) and 1.372 (Cu^{2+})	1.16 (Na$^+$) and 0.87 (Cu^{2+})	7.333 ± 0.04	350.0 ± 15.0	1.89 x10^{-3} ± 4.17 x10^{-5}
Zeolite 5A (Si/Al=1.0, Na$^+$, and Cu^{2+})		80CuNa5A	80% Cu^{2+} and 20% Na$^+$	0.93 (Na$^+$) and 1.372 (Cu^{2+})	1.16 (Na$^+$) and 0.87 (Cu^{2+})	8.015 ± 0.03	283.0 ± 15.0	8.14 x10^{-4} ± 4.27 x10^{-7}

Table 6.2 The induction and recovery times of modified zeolites, dPPV, and composites

Sample	Vapor type	Induction Time, T_i (min) at Vapor Concentration of					Recovery Time, T_r (min) at Vapor Concentration of				
		10	30	300	3000	30000	10	30	300	3000	30000
dPPV	acetone	15 ± 0.3	15 ± 0.6	18 ± 0.8	20 ± 0.5	35 ± 0.2	11 ± 0.1	11 ± 0.2	13 ± 0.5	13 ± 0.2	20 ± 1.0
80CuNaY		-	22 ± 0.5	27 ± 1.0	34 ± 0.8	40 ± 2.0	-	10 ± 3.0	12 ± 2.0	20 ± 0.3	30 ± 2.0
80CuNaMOR		19 ± 1.0	17 ± 1.0	20 ± 3.0	27 ± 2.0	35 ± 2.0	10 ± 4.0	14 ± 1.0	16 ± 2.0	18 ± 1.0	22 ± 1.0
80CuNa5A		-	15 ± 1.0	20 ± 2.0	25 ± 1.0	30 ± 2.0	-	13 ± 1.0	14 ± 2.0	15 ± 0.8	20 ± 1.0
dPPV_|90|80CuNaY		17 ± 2.0	18 ± 1.0	20 ± 2.0	30 ± 1.0	34 ± 2.0	12 ± 2.0	12 ± 3.0	15 ± 1.0	18 ± 2.0	24 ± 2.0
dPPV	methanol	20 ± 1.0	26 ± 0.5	28 ± 1.0	30 ± 0.5	38 ± 1.0	12 ± 2.0	13 ± 1.0	14 ± 2.0	16 ± 1.0	22 ± 0.5
80CuNaY		24 ± 2.0	25 ± 1.0	30 ± 2.0	40 ± 1.0	45 ± 1.0	13 ± 1.0	15 ± 0.5	20 ± 0.7	25 ± 0.2	28 ± 0.8
80CuNaMOR		21 ± 1.0	24 ± 1.0	28 ± 0.5	34 ± 1.0	40 ± 2.0	12 ± 1.0	14 ± 0.6	15 ± 2.0	20 + 2.0	24 + 1.0
80CuNa5A		-	23 ± 1.0	26 ± 1.0	33 ± 2.0	40 ± 2.0	-	13 ± 2.0	14 ± 1.0	17 ± 2.0	23 ± 1.0
dPPV_|90|80CuNaY		22 ± 1.0	26 ± 0.8	28 ± 2.0	31 ± 0.2	36 ± 1.0	13 ± 1.0	14 ± 1.0	15 ± 2.0	20 ± 0.8	26 ± 1.0
dPPV	n-heptane	14 ± 1.0	14 ± 2.0	16 ± 1.0	20 ± 0.8	23 ± 1.0	10 ± 0.5	10 ± 1.0	10 ± 0.5	10 ± 0.1	14 ± 2.0
80CuNaY		-	23 ± 1.0	24 ± 1.0	25 ± 1.0	30 ± 2.0	-	13 ± 2.0	14 ± 1.0	15 ± 2.0	20 ± 1.0
80CuNaMOR		-	22 ± 1.0	23 ± 1.0	23 ± 1.0	27 ± 1.0	-	12 ± 2.0	13 ± 1.0	13 ± 2.0	17 ± 1.0
80CuNa5A		-	17 ± 0.5	21 ± 2.0	22 ± 2.0	26 ± 1.0	-	11 ± 1.0	11 ± 2.0	12 ± 1.0	16 ± 1.0
dPPV_|90|80CuNaMOR		15 ± 1.0	16 ± 1.0	20 ± 1.0	21 ± 2.0	25 ± 0.5	10 ± 1.0	11 ± 0.5	11 ± 1.0	12 ± 1.0	15 ± 1.0

Table 6.3 The response and sensitivity of modified zeolites, dPPV, and composites

* The response and sensitivity of gas sensing materials at vapor concentration of 30000 ppm

Sample	Chemical Vapor	Response (S/cm)*	Sensitivity*	Minimum Vapor Concentration (ppm)
80CuNaY		$6.42 \times 10^{04} \pm 2.02 \times 10^{05}$	$4.87 \times 10^{-01} \pm 2.16 \times 10^{-02}$	9
80CuNaMOR		$2.60 \times 10^{-04} \pm 8.44 \times 10^{-05}$	$1.71 \times 10^{-01} \pm 3.06 \times 10^{-03}$	25
80CuNa5A	acetone	$2.48 \times 10^{-05} \pm 4.35 \times 10^{-06}$	$1.24 \times 10^{-01} \pm 1.95 \times 10^{-02}$	26
dPPV		$9.15 \times 10^{-02} \pm 8.76 \times 10^{-02}$	$4.42 \pm 8.42 \times 10^{-01}$	4
dPPV_[90]80CuNaY		$1.19 \times 10^{-01} \pm 7.44 \times 10^{-03}$	$4.93 \pm 6.96 \times 10^{-02}$	4
80CuNaY		$6.57 \times 10^{-04} \pm 4.03 \times 10^{-05}$	$7.90 \times 10^{-01} \pm 2.15 \times 10^{-02}$	5
80CuNaMOR		$3.03 \times 10^{-04} \pm 5.27 \times 10^{-06}$	$2.10 \times 10^{-01} \pm 1.77 \times 10^{-01}$	6
80CuNa5A	methanol	$1.71 \times 10^{-04} \pm 6.58 \times 10^{-06}$	$1.83 \times 10^{-01} \pm 2.41 \times 10^{-04}$	32
dPPV		$9.46 \times 10^{-02} \pm 2.05 \times 10^{-03}$	$5.60 \pm 2.77 \times 10^{-01}$	2
dPPV_[90]80CuNaY		$2.11 \times 10^{-01} \pm 6.32 \times 10^{-03}$	$5.77 \pm 2.41 \times 10^{-01}$	2
80CuNaY		$-5.38 \times 10^{-05} \pm 4.17 \times 10^{-06}$	$-9.31 \times 10^{-02} \pm 3.06 \times 10^{-03}$	13
80CuNaMOR		$-2.96 \times 10^{-04} \pm 2.22 \times 10^{-05}$	$-1.35 \times 10^{-01} \pm 2.93 \times 10^{-02}$	6
80CuNa5A	n-heptane	$-3.16 \times 10^{-05} \pm 7.06 \times 10^{-06}$	$-8.78 \times 10^{-02} \pm 2.25 \times 10^{-03}$	13
dPPV		$-3.26 \times 10^{-02} \pm 1.76 \times 10^{-02}$	$-3.93 \times 10^{-01} \pm 1.54 \times 10^{-02}$	4
dPPV_[90]80CuNaMOR		$-1.57 \times 10^{-03} \pm 2.56 \times 10^{-04}$	$-3.64 \times 10^{-01} \pm 1.50 \times 10^{-02}$	5